© 2015. Published by The Company of Biologists Ltd | The Journal of Experimental Biology (2015) 218, 2136-2142 doi:10.1242/jeb.117325

RESEARCH ARTICLE

The function of resilin in honeybee wings

Yun Ma, Jian Guo Ning, Hui Lan Ren*, Peng Fei Zhang and Hong Yan Zhao

ABSTRACT

The present work aimed to reveal morphological characteristics of worker honeybee (*Apis mellifera*) wings and demonstrate the function of resilin on camber changes during flapping flight. Detailed morphological investigation of the wings showed that different surface characteristics appear on the dorsal and ventral side of the honeybee wings and the linking structure connecting the forewing and hindwing plays an indispensable role in honeybee flapping flight. Resilin stripes were found on both the dorsal and ventral side of the wings, and resilin patches mostly existed on the ventral side. On the basis of resilin distribution, five flexion lines and three cambered types around the lines of passive deformation of the coupled-wing profile were obtained, which defined the deformation mechanism of the wing along the chord, i.e. concave, flat plate and convex. From a movie obtained using high-speed photography from three orthogonal views of free flight in honeybees, periodic changes of the coupled-wing profile were acquired and further demonstrated that the deformation mechanism is a fundamental property for variable deformed shapes of the wing profile during flapping flight, and, in particular, the flat wing profile achieves a nice transition between downstrokes and upstrokes.

KEY WORDS: Morphology, Resilin, Camber, Fluorescence microscopy, Deformation mechanism, *Apis mellifera*

INTRODUCTION

Research on the structural characteristics and material properties of the insect wings is essential for understanding aerodynamic performance and maneuverability, which have fascinated biologists and physicists for many years. Many previous studies on flapping insect wings relied on the assumption that the wings act as rigid, non-deformable flat plates (Combes and Daniel, 2003b; Ho et al., 2003; Shyy et al., 2008; Vanella et al., 2009). However, an insect wing is composed of a corrugated network of relatively stiff veins and thin strained membranes, constituting a tightly three-dimensional structure. Bats and birds can actively control the flexibility and shape of their wings; however, insects have little ability to modulate wing properties and their excellent flapping flight depends on the wing base control (Ennos, 1988) and passive deformations of the wings (Wootton, 1992). High-speed photography has shown that most insects are able to produce effective aerodynamic forces for hovering and forward flight during a single flapping cycle (Weis-Fogh, 1973; Ellington, 1984a,b; Ennos, 1988), reversing the dorsal and ventral surfaces through rotating the wings about their longitudinal axis by more than 90 deg between half-strokes (Ennos, 1988).

Beijing Institute of Technology, State Key Laboratory of Explosion Science and Technology, 5 South Zhongguancun Street, Haidian District, Beijing 100081, People's Republic of China.

*Author for correspondence (huilanren@bit.edu.cn)

Received 25 November 2014; Accepted 6 May 2015

The flexibility of biological materials probably results in these passive deformations, which appear to be predictable as well as beneficial for the insect's flight (Wootton, 1981). How the instantaneous wing profile of the locust varies through the wingbeat at different wing spanwise locations has been provided, indicating that changes in camber through a wingbeat are fairly consistent for the hindwing both within and between individuals (Walker et al., 2009). In tests, cambered wings can produce higher lift and higher maximum lift to drag ratio than flat or rigid ones (Vogel, 1967; Dudley, 1987; Mountcastle and Daniel, 2009; Young et al., 2009). Numerical simulations have shown that the flexible torsion of the wings contributes to the stability of flapping flight; without this torsional flexibility, the oscillation of the thorax will cause flight instability for the insect model (Senda et al., 2012).

How can insects so superbly accomplish flexible deformation of their wings? Resilin, a rubber-like protein (Weis-Fogh, 1960), is probably the answer to this question. In the first description of resilin, it was viewed as energy-storing tendons in dragonflies and elastic wing hinges in locusts (Weis-Fogh, 1960). Then it was found in the feeding pump of *Rhodnius prolixus* (Bennet-Clark, 1963), and was described as the elastic spring that powers the agile flea leg with high catapulting speed (Bennet-Clark and Lucey, 1967). With thousands of flapping cycles, insect wings should be adapted for reversible failure in response to excess loads (Newman and Wootton, 1986); thus, resilin's high flexibility and capacity for storing energy (energy loss of less than 5% over a wide range of frequencies; Jensen and Weis-Fogh, 1962) mean that it is capable of preventing the wings from permanent material and structural damage. The distribution pattern of resilin in beetle wings correlates with its particular folding mechanism, requiring extra elasticity in wing folds (Haas et al., 2000a,b). But until now, few studies (Gorb, 1999; Lehmann et al., 2011; Donoughe et al., 2011; Mountcastle and Combes, 2013) have focused on resilin's function in wing deformation during flapping flight.

In our study, we used microscopy techniques and high-speed photography to examine the distribution pattern and function of resilin in the worker honeybee (*Apis mellifera* Linnaeus 1758) wing and to illustrate how resilin operates in the deformation of the wings during flapping flight.

RESULTS

Wing morphology

A worker honeybee *A. mellifera* has two pairs of wings, each pair of which includes a forewing and a hindwing (Fig. 1). Fig. 2 shows morphological characteristics of forewing and hindwing surfaces. In general, the area of the forewing is larger than that of the hindwing. The dorsal side of the forewing is a relatively flat surface (Fig. 2B,D), although there are abundant hairs on both sides of the wing. In contrast, veins protrude from the forewing ventrally (Fig. 2C,D). The hindwing has similar features. Unlike dragonfly wings, which are crisscrossed by cross-veins and longitudinal veins with a large quantity of membrane cells, the venation of honeybee wings is not complicated. In the forewing and hindwing, four

The Journal of Experimental Biology

The Journal of Experimental Biology (2015) 218, 2136-2142 doi:10.1242/jeb.117325

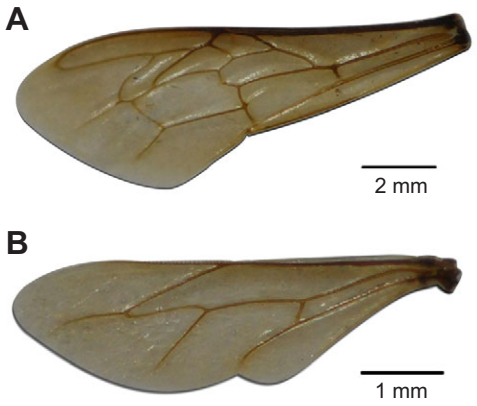

Fig. 1. Forewing and hindwing of a worker honeybee (*Apis mellifera*). Images of the forewing (A) and hindwing (B) were captured by a Canon EOS 550D camera.

longitudinal veins, including the leading vein and the trailing vein, are longitudinally arranged and only the costal vein spreads from wing base to wing tip. Vein branches always run obliquely to the hind margin, which would be inclined to oppose the longitudinal flexion required for camber changes (Wootton, 1981).

What is noteworthy is the hook structure (HS) (Fig. 2E and Fig. 3A) of the hindwing and the membrane-rolling structure (MRS) (Fig. 3) of the forewing, both of which firmly connect the forewing and hindwing. In total, there are 21 hooks emerging from the vein joint on the costa of the hindwing (position 1, Fig. 2E) and then disappearing at the end of the costa of the hindwing (position 2, Fig. 2E). As seen from the magnified hook (Fig. 3A), each hook is composed of two 'spars', which constitute a V-shape joint (Fig. 3A,C). One spar is embedded in the leading edge of the hindwing and the other is hooked to the trailing edge of the forewing. The MRS of the forewing corresponds to the HS of the hindwing. The membrane at the end of the trailing edge of the forewing firstly climbs up and then rolls to the ventral side, through which the MRS is developed. Scanning electron microscopy (SEM) images of a cross-section of the MRS (Fig. 3B) reveal a fantastic spiral (Fig. 3B,C). The length of the MRS along the longitudinal direction of the wing is a little greater than that of the HS, which enables all hooks to attach to the MRS and stops them slipping from it during longitudinal relative motion between the forewing and hindwing. The linking pattern between the HS and MRS is illustrated in Fig. 3C.

According to SEM and fluorescence microscopy (FM) images of honeybee wings, two main types of the vein joint occur in the forewing and hindwing: mobile and immobile. The immobile type allows flexible articulation of veins without an imbued resilin patch (Fig. 4A,B), while the mobile type allows articulation with imbued resilin (Fig. 4C,D). Analysis of the resilin distribution in the wings (Fig. 5A) revealed one patch in the hindwing and five resilin-embedded flexible joints in the forewing (except the resilin patch at position C in Fig. 5A, which is too far from the vein articulation), including the flexible joint on the medio-cubital (1m-cu) cross-vein. Analogously, resilin occurs at the same position on the 1m-cu vein in the bumblebee wing (Mountcastle and Combes, 2013). The other joints without imbued resilin could be classified as immobile.

Distribution of resilin patches and resilin stripes

The presence of resilin in honeybee wings was revealed by FM in the UV band. There was autofluorescence of resilin at positions with necessary flexibility, such as the wing base, where strong fluorescence was observed (Fig. 5G), locations at or near vein joints (Fig. 5B,C,D) and connections of veins and membranes (Fig. 5E,F). As the variable thickness of the wing would result in a blurred FM image caused by numerous parts being out of focus, we only focused on the specific position showing fluorescence of the resilin patch or the resilin stripe.

Please note that, because of the age of the FM equipment and variable thickness of specimens, we could not capture sharp micrographs with clear larger areas, and the greater the magnification, the less clear the areas were. This meant that most of the FM images had to be obtained under 5× and 10× magnification. Once the corresponding equipment has been upgraded, we will conduct more detailed fluorescence experiments under higher magnification.

The autofluorescence of the wing base mainly occurred at the position that is connected to the honeybee body. The wing base showed obvious fluorescence (Fig. 5G), much stronger than that of other positions. Likewise, the resilin patch in the wing base was generally larger than those of other positions.

On the ventral side of the forewing, FM revealed six resilin patches on cross-veins and some bright resilin stripes along veins. Similar to the observation that, in dragonfly wings, resilin is mostly in vein joints where cross-veins meet longitudinal veins (Donoughe et al., 2011), the rubber-like protein of honeybee wings might also act as an elastic element close to the mobile vein joints (Fig. 5A,B,C,D,F). Three of the six resilin patches were distributed

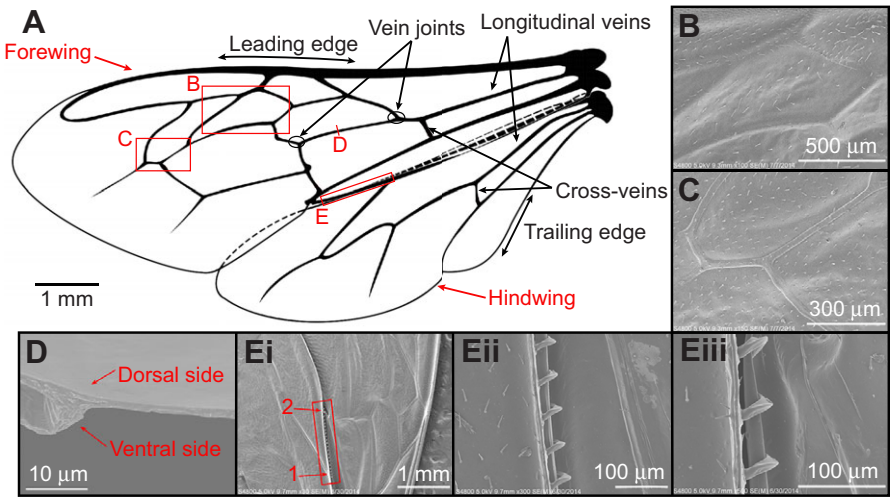

Fig. 2. Wing morphology of a worker honeybee (dorsal side). (A) A pair of coupled wings. Dashed lines illustrate the parts of the hindwing beneath the forewing. Areas labeled B–E refer to the four specific positions on the coupled wings and relate to the panels below. (B) Scanning electron microscopy (SEM) image of details of the dorsal surface at position B of the forewing. (C) SEM image of details of the ventral surface at position C of the forewing. (D) SEM image of the cross-section of a vein at position D of the forewing. (Ei–iii) SEM images of the hook structure (HS) at position E under different magnifications (ventral side). 1, vein joint on the costa; 2, end of the costa.

The Journal of Experimental Biology (2015) 218, 2136-2142 doi:10.1242/jeb.117325

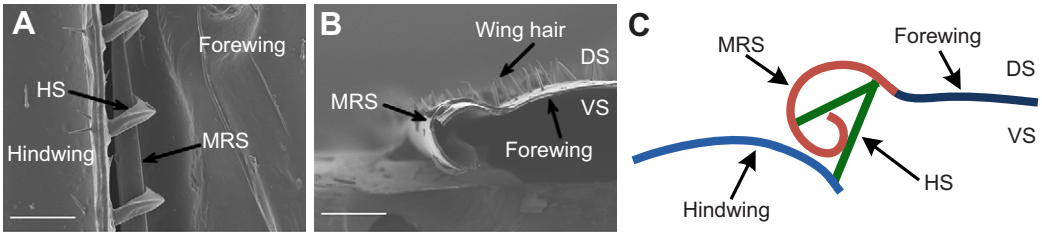

Fig. 3. SEM images and illustration of the linking structure. (A) SEM image of the HS of the hindwing. Wings are shown from the ventral side. Scale bar represents 50 μm. (B) SEM image of a cross-section of the membrane-rolling structure (MRS) of the forewing. Scale bar represents 50 μm. DS, dorsal side; VS, ventral side. (C) Schematic diagram of the cross-section of the HS and MRS connected together, which we call the linking structure (LS). The red and green lines represent the MRS and HS, respectively. The red with the dark blue line represents the forewing. The light blue with the green line represents the hindwing.

in the middle part of the forewing, one in the basal part and the other two in the distal part (Fig. 5A). On the dorsal side of the forewing, several very faint resilin patches (Fig. 5B,D) and some resilin stripes were observed, but considering the low level of the fluorescence, these patches were not marked in Fig. 5. Similarly, one resilin patch on the dorsal side of the hindwing and a few resilin stripes on both sides of the hindwing were revealed by FM. Interestingly, not all resilin stripes existed on both sides of veins, and more bright resilin stripes (Fig. 5E,F) were located on only one side (closer to the leading edge of the wing) of veins. The distribution of resilin in the HS and MRS is shown in Fig. 6. There are two resilin stripes on the MRS, with one (Fig. 6E, resilin stripe 1) located at the boundary position between the dorsal side and ventral side, and the other (Fig. 6E, resilin stripe 2) at the start position of the MRS (Fig. 6D,E).

High-speed photography of honeybee flapping flight

A high-speed camera system (Fig. 7) was used to capture clear and detailed shape changes of the honeybee wing profile from three views during flapping flight. The three columns of images in Fig. 8A present the wing deformations with a concave wing profile (ventral side is concave), a flat wing profile and a convex wing profile (ventral side is convex) from three different views, namely back, top and right side of the honeybee filmed (see supplementary material Movie 1).

DISCUSSION

Wing morphology

Venation

From the view point of morphology, both the dragonfly and honeybee have two pairs of wings. From the functional view point, the dragonfly still has two pairs of wings; in contrast, the honeybee has only one pair of wings, as the forewing and hindwing of the honeybee are connected together by the linking structure (LS) during flight, working as one pair of wings.

Marginal veins would significantly prevent cracks from propagating across membrane cells to tear the wing (Wootton, 1992); however, no vein exists on the edge of marginal areas of honeybee wings. The reason for this is probably that the absence of veins on the edge can reduce the weight of the wings to make the center of mass closer to the wing base, as well as keeping the flexibility of wing marginal areas, because the wings, especially the marginal areas, will be extremely rotated during stroke reversal according to close-up photos obtained using high-speed photography. An alternative explanation for the absence of marginal veins is that membrane stresses in marginal areas normally caused by external forces may not tear the honeybee wing, unlike dragonfly wings, which have a larger surface area. However, these are simply hypotheses for the absence of marginal veins on honeybee wings, which have not been tested. The latest research of Mountcastle and Combes (2014) showed that veins of the bumblebee wing are withdrawn to the proximal part of the wing, which makes the entire distal part unreinforced and more continuously flexible. This may allow the wing to buckle upon contact with an obstacle, presumably preventing wing damage due to collisions. The wing architecture of the closely related honeybee may perform a similar function to protect the wing.

Vein joint

We have known that several mobile vein joints occur in honeybee wings and that other vein joints are immobile (Fig. 4 and Fig. 5A). As indicated in Fig. 4C,D and Fig. 5A, the rubber-like resilin patches of the mobile joints are located along the chord of the wing, conferring flexibility on the wing chord. Mountcastle and Combes (2013) have tested the function of the bumblebee major flexible vein joint on the 1m-cu vein on chordwise flexibility, finding an average increase of 37.6±9.37% in chordwise flexural stiffness by splinting the 1m-cu joint. Therefore, the 1m-cu joint (Fig. 5A) on the honeybee wing may play an analogous role in chordwise wing flexibility. Moreover, considering the other mobile vein joints and LS, the influence of flexion lines of the honeybee wing on the chordwise deformation of the wing will be discussed below (see Discussion, ‘Functional role of resilin patches in wings’).

HS and MRS

The HS is an unexpected finding through SEM (Fig. 2Ei–iii and Fig. 3). Generally, it firmly connects the trailing edge of the forewing and the leading edge of the hindwing during honeybee rest

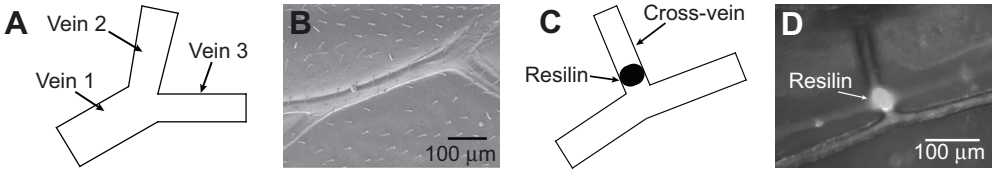

Fig. 4. Scheme and micrograph of two main types of vein joints of the honeybee wing. (A) Scheme of the immobile vein joint. (B) SEM image of the immobile joint without the imbued resilin patch. (C) Scheme of the mobile joint. (D) Fluorescence microscopy (FM) image of the mobile joint with the imbued resilin patch.

The Journal of Experimental Biology (2015) 218, 2136-2142 doi:10.1242/jeb.117325

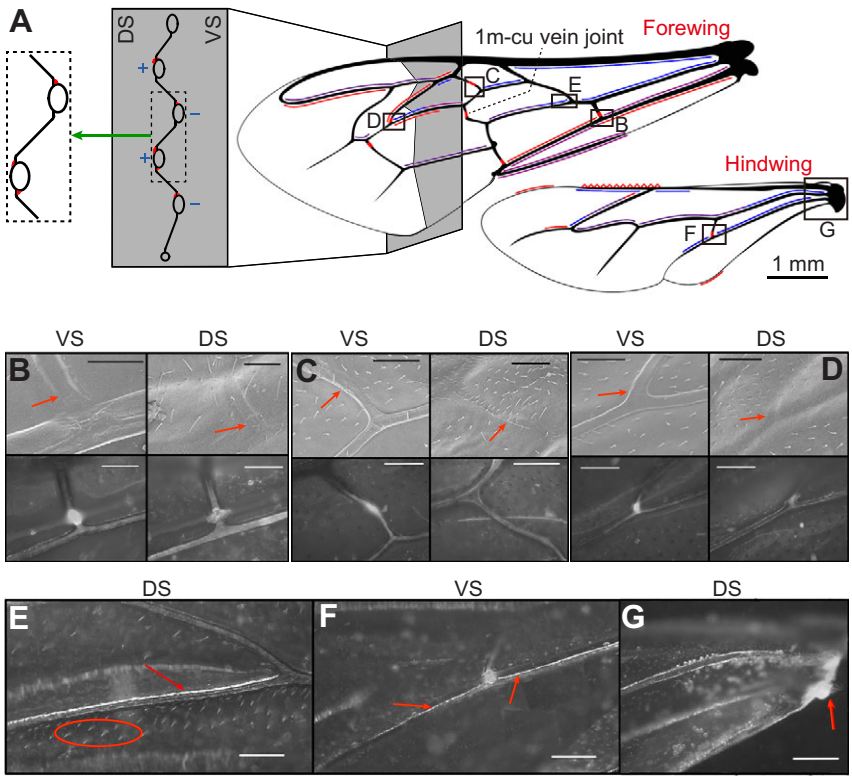

Fig. 5. The resilin distribution in a forewing and hindwing pair from a worker honeybee. Because of impurities on wing surfaces, dim and irregular fluorescent patches of FM images were neglected. Scale bars represent 100 μm. (A) Schematic diagram of the dorsal and ventral distribution of resilin patches on veins and resilin stripes on connections of veins and membranes. Red patches and lines represent the ventral distribution of resilin, blue lines represent the dorsal distribution of resilin, and purple lines mean that resilin exists at the same position on both the dorsal and ventral side of the wings. The corrugated structure illustrates the resilin distribution in the corrugated cross-section, with alternating '+' (mountains) and '–' (valleys). Areas labeled B–G relate to the panels below. (B–D) SEM (top) and FM (bottom) images of both the dorsal and ventral side of the wing at selected positions. Red arrows point to positions with resilin patches in SEM images. Strong resilin patches occurred on the ventral side of the wings, whereas very weak patches or no patch at all was present dorsally (so no resilin patch was marked on the dorsal side). (E) FM image of a resilin stripe on the dorsal side of the forewing. Wing hairs inside the red ellipse show the fluorescence and the red arrow points to a brightly fluorescent stripe. (F) FM image of one resilin patch and two resilin stripes on the hindwing. Red arrows point to resilin stripes. (G) FM image of a resilin patch at the base of the hindwing. The red arrow points to the resilin patch.

and flapping flight. But based on our observations, when the living space of honeybees is so narrow that their wings are in contact with their surroundings, the forewing and hindwing will be unhooked and overlapped, aligning parallel to the honeybee body axis. Every hook is composed of two spars, which constitute a V-shape joint (Fig. 3A,C). One spar is embedded in the leading edge of the hindwing and the other is hooked to the trailing edge of the forewing. The MRS of the forewing, whose cross-section is nearly a spiral (Fig. 3C), effectively opposes complex torsion due to the tension from the hindwing, and grasps the hindwing hooks. These HS and MRS form the LS and guarantee the steady connection (Fig. 3C) between the forewing and hindwing during flight. The LS functionally results in the rotation of the forewing and hindwing relative to each other, consequently functioning as a flexion line and surely relating to the development of camber (see Discussion, 'Functional role of resilin patches in wings'). That the outstanding mechanical behaviors of the LS depend on the material properties of the HS and MRS should be acknowledged. The HS and MRS show autofluorescence, which indicates the existence of resilin in these two structures, and the function of resilin in the HS and MRS will be discussed below.

Functional role of resilin stripes in wings

Because of the abrupt structure change of the connections between veins and membranes, stress is most likely to be concentrated at these connections, yet resilin, which exists at the connections, has a higher breaking strain and can bear greater deformation. For instance, the crack propagation of wing samples of locust *Schistocerca gregaria* (see videos in Dirks and Taylor, 2012) occurred away from the connections. Resilin stripes may therefore increase the fracture toughness of the connections, preventing cracks from propagating at positions of the structure with abrupt changes, even though there is no experimental evidence that resilin exists in the wings of *S. gregaria*.

The HS and MRS of the LS show obvious fluorescence in Fig. 6. We conclude that the hook is commonly in the hindwing plane when it is free (Fig. 6B); nevertheless, the hook appears to be rotated along the spar, which is embedded in the edge of the hindwing, when it is linked to the MRS (Fig. 6C). Deformed resilin in the hook may enable it to fix tightly to the MRS with the help of friction and the spiral structure of the MRS (Fig. 3C). For the MRS, twisted resilin stripes tend to resist forces applied by the hooks and maintain the original state of its spiral structure to hold the hooks. Hence, the

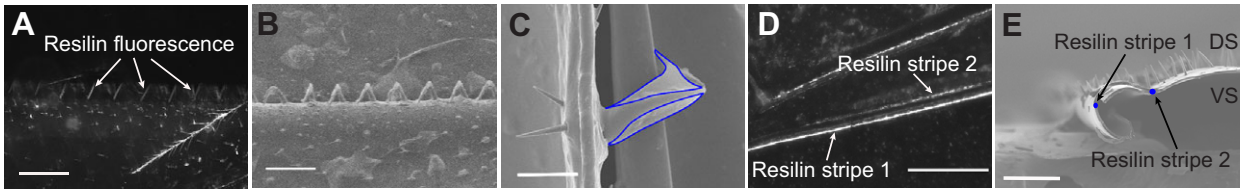

Fig. 6. Distribution of resilin in the HS and MRS. (A) FM image of the HS in the hindwing (ventral side). Scale bar represents 100 μm. (B) SEM image of the HS in the hindwing (dorsal side). Scale bar represents 100 μm. (C) SEM image of a hook with resilin patches surrounded by blue curves. Scale bar represents 20 μm. (D) FM image of the MRS in the forewing (ventral side). Scale bar represents 150 μm. (E) SEM image of the cross-section of the MRS. The two blue dots are the cross-sections of resilin stripes 1 and 2. Scale bar represents 50 μm.

The Journal of Experimental Biology (2015) 218, 2136-2142 doi:10.1242/jeb.117325

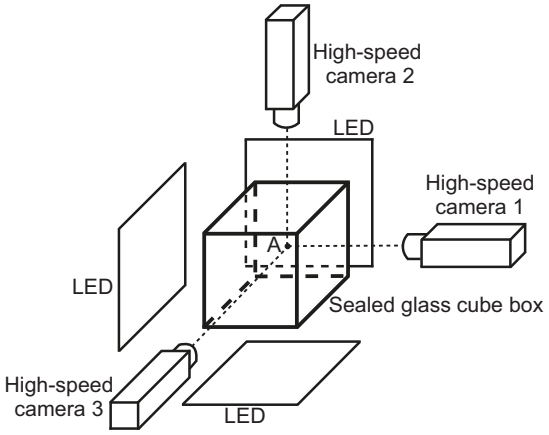

Fig. 7. Schematic diagram of the system for photographing the free flight of the honeybee. In order to construct a bright white background for three-view photography, LED panels located at the three view positions of the sealed glass cube box were used to provide white light. The optical axes of the three cameras were aligned passing through the volumetric center A of the glass box.

forewing and hindwing can be linked by the HS and MRS through the inherent function of resilin.

Functional role of resilin patches in wings

From a functional point of view, the insect wing can be divided into two kinds of components: deformation-restricting areas supporting the whole wing and restraining the distortion of the deformable areas, and passively deformable areas bearing considerable passive shape changes when subjected to inertial and aerodynamic forces (Wootton, 1981). There are a series of tiny steering muscles located in the thorax of the blowfly (*Calliphora vicina*) (Wisser and Nachtigall, 1984), several of which affect the kinematic variables of the wing such as stroke trajectory and stroke amplitude (Heide and Götz, 1996; Lehmann and Götz, 1996; Tu and Dickinson, 1996), and the thorax of the honeybee is potentially similar to that of *C. vicina*. In the honeybee wings, the forces that are exerted by the steering muscles and that drive the wing to perform flapping flight are transmitted from the wing base to the wing tip by its supporting components, leading the wing to be distorted during maneuvering flight. As a result, the active control and wing architecture play an indispensable role in regulating kinematics and passive deformation of the wing.

The wing base, controlled by the steering muscles of the honeybee thorax, stands the highest stress over the whole wing during one flapping cycle. The occurrence of the rubber-like resilin protein at this position suggests that it increases the breaking strain of the base, which probably prevents material fatigue (Haas et al., 2000a). Resilin acts as a rubber-like material, possessing outstandingly high resilience and impact-absorbing capacity and showing 95% elastic efficiency (Lv et al., 2010) with little loss of elastic potential energy due to wing elasticity (Lehmann et al., 2011), so another indispensable function of resilin in the wing base may be to perform the storage and release of energy for flapping flight.

Based on one resilin patch in the hindwing (flexion line 1 in Fig. 9), six resilin patches in the forewing (flexion lines 3–5 in Fig. 9) and the LS (flexion line 2 in Fig. 9) of the forewing and hindwing, we conclude that one coupled wing contains in total five flexion lines, allowing it to flex along the chord. The flexion lines are axes of the wing profile deformation during flapping flight, which most likely increase the chordwise flexibility and make the wing return to its initial position promptly after the elastic deformation by the twisted or bended resilin springs when no

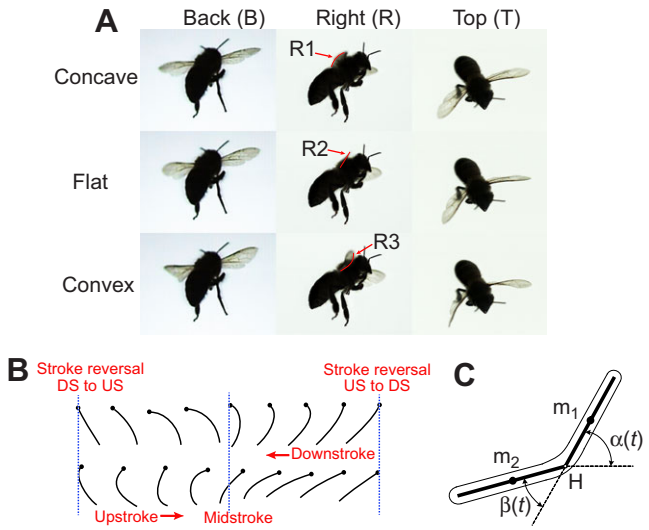

Fig. 8. Deformation of the coupled-wing profile. (A) Transition from a concave to a convex camber profile during supination. The images were recorded by three high-speed cameras. Camera shutter time was 50 μs and frames were recorded at 200 μs. The three columns of images present the synchronous wing deformation of three orthogonal views (namely back, top and right side of the honeybee) filmed. The time interval between the concave and the flat profile was 200 μs and time interval between the flat and the convex profile was 400 μs. Red arrows and thin red curves highlight three wing profile cases (see Fig. 9) in the supination. The process of wing deformation during flight can be seen in supplementary material Movie 1. (B) Alteration in the shape of the coupled-wing profile during a flapping cycle. Shape changes of the coupled-wing profile during downstroke (top) and upstroke (bottom) are shown, including concave, flat plate and convex. US and DS represent upstroke and downstroke, respectively. (C) The two-link model (Vanella et al., 2009). The two links, m_1 and m_2, which are rigid body links, are connected by the torsional spring H with torsion constant κ, which is similar to the flexion line. They are covered by aerodynamic surfaces to function as the airfoil. The variables $\alpha(t)$ and $\beta(t)$ are generalized coordinates to describe the rotation motion of the two rigid links relative to each other (see details in Vanella et al., 2009).

external force is acting (Gorb, 1999). Camber is developed by the supporting parts and passively deformable regions of the wing (Wootton, 1981). To a certain degree, the existence of several parts separated by flexion lines is a necessary condition for the development of camber of the coupled wing along the chordwise direction. Here, the flexion lines are just hypothesized based on the distribution of resilin patches, the relative positions of wing veins and the observed wing deformations during flight, conducive to understanding the coupled-wing deformation. As shown in Fig. 9, the three cambered cases (case 1, concave; case 2, flat plate; case 3, convex) clearly indicate how the shape of the wing profile changes as a result of the presence of the flexion lines.

Supplementary material Movie 1 of honeybee flapping flight clearly shows the basal vein movement (right and top view of the movie), which rotates the costa to drive the flapping movement of the coupled wing and regulate the wing deformation with camber changes. As has been assumed by others (Boettiger and Furshpan, 1952; Miyan and Ewing, 1985), torque is actively applied by wing base sclerites, which rotate the leading edge of the wing. The wingstroke of an insect is typically divided into four kinematic phases: downstroke, upstroke and two stroke reversals (supination and pronation) (Dickinson et al., 1999). During the downstroke, as seen in the movie, the coupled wing sweeps through the air and, as the trailing edge is put under tension when the wing is pulled forward, compressive forces in the radial veins are induced by the curvature of the trailing edge (Wootton, 1995; Walker et al., 2009), leading to

The Journal of Experimental Biology (2015) 218, 2136-2142 doi:10.1242/jeb.117325

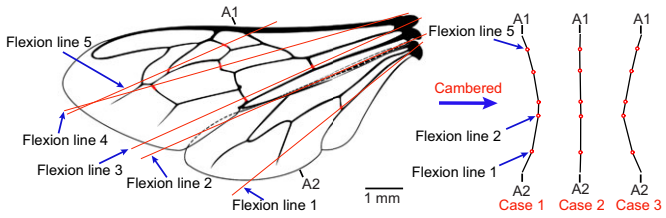

Fig. 9. Possible flexion lines composed of resilin patches or LS in the coupled wing of a worker honeybee. The HS, through which the forewing and hindwing can rotate relative to the each other, is viewed as a flexion line (in red, flexion line 2), while resilin, an ideal material for making elastic hinges that can endure repeated periodic stress (Weis-Fogh, 1960; Bennet-Clark, 2007), constitutes the other flexion lines. The majority of the flexion lines pass through the wing base, to some degree being under the control of the wing base. Cases 1–3 represent three cambered types of passive deformation of the wing around the flexion lines, which are concave (ventral side is concave), flat plate and convex (ventral side is convex).

Euler buckling of the radial veins (Wootton, 1995). This is presumably the main source of the camber during the downstroke. At this moment, the wing is cambered with a concave ventral side (R1 in Fig. 8A), as in case 1 in Fig. 9. When the downstroke reverses to the upstroke (supination), first the costa of the forewing is rotated under the control of the wing base and then the maximum torsion of the wing can be observed with camber reversal from concave (case 1 in Fig. 9, R1 in Fig. 8A) to convex (case 3 in Fig. 9, R3 in Fig. 8A). The flat wing profile (case 2 in Fig. 9, R2 in Fig. 8A) appears between the concave and convex profiles, being essential for camber reversal. At the beginning of the upstroke, a marked angle (right and top view of the movie) between the forewing and hindwing at the basal and proximal part, probably caused by forewing torsion, is captured, creating a single strongly cambered aerofoil (Wootton, 1981). This shows the function of the LS as a flexion line (flexion line 2 of case 3, Fig. 9) to facilitate torsion, and might be a pronounced feature of the coupled-wing deformation during flight. Compared with camber curvature of the wing in the downstroke, the curvature in the upstroke is larger, potentially owing to the LS and greater forewing torsion observed in the movie. At the end of the upstroke, the costas of right and left forewing are nearly parallel to each other (top view of the movie), and during pronation the costa of the forewing is first rotated, leading the wing to be involved in the downstroke. Then, the convex camber reverses to the concave one. Throughout the whole cycle of free flight of the honeybee, the 'concave' and 'convex' cases (case 1 and 3 in Fig. 9) reveal the formation of the camber and are maintained during the upstroke and downstroke, according to the movie. It is worth noting that the 'flat plate' case (case 2 in Fig. 9) is specifically associated with stroke reversal of the coupled wing.

The intact shape changes of the coupled-wing profile of the honeybee during a flapping cycle are summarized in Fig. 8B. The wing camber is concave during the downstroke; in contrast, it is convex during the upstroke. It should be highlighted that the concave camber generated throughout the downstroke is evidence for the operation of the 'umbrella effect' observed by other researchers (Wootton, 1995; Wootton et al., 2000, 2003). The flat wing profile appears at stroke reversal and enables the indispensable transition for camber reversal. Please note that there is another possible wing profile which may be equal to the flat type, i.e. S-shape, as at the start of the supination, the costa of the forewing is rotated into upstroke and meanwhile the other part of the wing is still maintained in concave camber, thus probably generating the S-shape, which has not been verified by the test. If this is confirmed by a more precisely conducted experiment, the S-shape type will surely be shown to facilitate the stroke reversal.

Resilin may impact on both the flexural stiffness distribution and aerodynamic performance of the wings, even though the material property of membranes and veins cannot be neglected. The distribution pattern of resilin patches of the honeybee wings indicates that flexion perhaps occurs more easily in the chordwise direction, while the relatively rigid longitudinal veins, not interrupted by resilin patches, will resist spanwise flexion. Flexural stiffness along the spanwise direction of insect wings is generally 1 or 2 orders of magnitude larger than flexural stiffness along the chordwise direction (Combes and Daniel, 2003a). For researchers, the influence of stiffness distribution on aerodynamic characteristics is one of the biggest concerns in the field of insect flapping flight. Vanella et al., (2009) have explored the aerodynamic performance of a flexible wing during hovering. They put forward a simplified computational model (Fig. 8C) to show the influence of wing flexibility on hovering, which demonstrates that aerodynamic performance can be enhanced by wing flexibility. Additionally, the flexible structure is conducive to reinforcing load-lifting capacity, power efficiency and wing propulsion efficiency (Mountcastle and Combes, 2013; Liu et al., 2013; Zhu, 2007), and deformations of insect wings bring about a camber effect that may regulate the magnitude of lift and drag ratio and control the alteration of aerodynamic forces (Walker et al., 2009; Zhao et al., 2010). Therefore, we believe that resilin, largely by determining the flexibility of the wings, is a principal reason why the honeybee and even insects in general are able to excellently perform flapping flight. This mechanism is helpful not only for understanding the essence of insect flight but also for researchers and engineers who devote themselves to designing bionic wings and improving the aerodynamic performance of micro-air-vehicles (MAVs).

MATERIALS AND METHODS

Specimen collection

A representative of honeybee families was used. Worker honeybees (*A. mellifera*) were obtained from the Bee Research Institute, Chinese Academy of Agricultural Sciences. The spanwise forewing and hindwing length were, respectively, 9.35 and 6.37 mm.

Fluorescence microscopy

For fluorescence microscopy, two pairs of wings were cut off from one freshly killed honeybee. They were cleaned in 75% ethanol, to wipe out dust as much as possible and improve the sharpness of images. After drying the four wings, they were mounted between two coverslips to flatten them and observed in a fluorescence microscope (Leica DMI 6000B, Leica Microsystems, Germany) in one of three bands of wavelengths: blue (excitation 470–540 nm, emission 475–575 nm), green (excitation 515–560 nm, emission 590 nm) and UV bands (excitation 340–380 nm, emission 425 nm). Generally, insect cuticle has an autofluorescence at wavelengths from blue–green to deep-red; however, resilin in biological structures shows this trait only at a very narrow band of wavelength of approximately 400 nm (Andersen et al., 1964). Consequently, there was no need to use immune labeling and other treatments to reveal the autofluorescence of resilin, keeping specimens as native as possible. The lab temperature and humidity were maintained at 25°C and 60%, respectively.

We conducted a detailed investigation on four sides of the wings: the dorsal side of the left forewing, the ventral side of the right forewing, the dorsal side of the left hindwing and the ventral side of the right hindwing.

SEM

For SEM, two pairs of the coupled forewing and hindwing (dorsal side and ventral side up, respectively) and two samples with a transverse section of the forewing and hindwing were dry mounted on holders and sputter-coated with gold about 7 nm thick. Sputter-coating can prevent wings from being non-conducting and help to create sharp SEM images. The samples were observed in a Hitachi S-4800 scanning electron microscope (Hitachi, Ltd., Japan) at 5 kV.

High-speed photography

In order to photograph profile changes of the honeybee coupled wing during free flight, a camera system (Fig. 7) was assembled, including three high-speed cameras [Olympus i-Speed 3 (Olympus Corporation, Japan), Photron SA4 and Photron SA5 (Photron, Japan)], an LED panel and a sealed glass box (hand-made). The cameras were focused on point A (the volumetric center of the glass box), and when a honeybee flew to regions near the point A, the cameras were synchronously triggered to capture the flapping behavior. Shutter time of the three cameras was set at 50 µs and frames were recorded at 200 µs.

Acknowledgements

We thank professor Liu Zhanwei and his masters degree candidate Shi Wenxiong (Beijing Institute of Technology, Beijing, China) for providing the optical microscope, professor Huo Bo and his masters degree candidate Li Shu'na (Beijing Institute of Technology) for providing the fluorescence microscope and helping to analyze the FM results, and Guo Haikun (Bee Research Institute, Chinese Academy of Agricultural Sciences, Beijing, China) for providing living worker honeybees.

Competing interests

The authors declare no competing or financial interests.

Author contributions

Y.M. contributed to the experimental design, collection and analysis of the results and writing the manuscript. J.G.N. and H.L.R. contributed with discussion of results and comments on the manuscript. P.F.Z. and H.Y.Z. contributed to designing the camera system and discussion of the results.

Funding

This work was supported by the National Natural Science Foundation of China [grant number 11172045].

Supplementary material

Supplementary material available online at
http://jeb.biologists.org/lookup/suppl/doi:10.1242/jeb.117325/-/DC1

References

Andersen, S. O. and Weis-Fogh, T. (1964). Resilin. A rubberlike protein in arthropod cuticle. *Adv. Insect Physiol.* **2**, 1-65.
Bennet-Clark, H. C. (1963). Negative pressures produced in the pharyngeal pump of the bloodsucking bug, *Rhodnius prolixus*. *J. Exp. Biol.* **40**, 223-229.
Bennet-Clark, H. (2007). The first description of resilin. *J. Exp. Biol.* **210**, 3879-3881.
Bennet-Clark, H. C. and Lucey, E. C. A. (1967). The jump of the flea: a study of the energetics and a model of the mechanism. *J. Exp. Biol.* **47**, 59-76.
Boettiger, E. G. and Furshpan, E. (1952). The mechanics of flight movements in Diptera. *Biol. Bull.* **102**, 200-211.
Combes, S. A. and Daniel, T. L. (2003a). Flexural stiffness in insect wings. I. Scaling and the influence of wing venation. *J. Exp. Biol.* **206**, 2979-2987.
Combes, S. A. and Daniel, T. L. (2003b). Into thin air: contributions of aerodynamic and inertial-elastic forces to wing bending in the hawkmoth *Manduca sexta*. *J. Exp. Biol.* **206**, 2999-3006.
Dickinson, M. H., Lehmann, F.-O. and Sane, S. P. (1999). Wing rotation and the aerodynamic basis of insect flight. *Science* **284**, 1954-1960.
Dirks, J.-H. and Taylor, D. (2012). Veins improve fracture toughness of insect wings. *PLoS ONE* **7**, e43411.
Donoughe, S., Crall, J. D., Merz, R. A. and Combes, S. A. (2011). Resilin in dragonfly and damselfly wings and its implications for wing flexibility. *J. Morphol.* **272**, 1409-1421.
Dudley, T. R. (1987). The mechanics of forward flight in insects. PhD thesis, University of Cambridge, UK.
Ellington, C. P. (1984a). The aerodynamics of hovering insect flight. III. Kinematics. *Philos. Trans. R. Soc. B Biol. Sci.* **305**, 41-78.
Ellington, C. P. (1984b). The aerodynamics of hovering insect flight. VI. Lift and power requirements. *Philos. Trans. R. Soc. B Biol. Sci.* **305**, 145-181.
Ennos, A. R. (1988). The importance of torsion in the design of insect wings. *J. Exp. Biol.* **140**, 137-160.
Gorb, S. N. (1999). Serial elastic elements in the damselfly wing: Mobile vein joints contain resilin. *Naturwissenschaften* **86**, 552-555.
Haas, F., Gorb, S. and Blickhan, R. (2000a). The function of resilin in beetle wings. *Proc. R. Soc. B Biol. Sci.* **267**, 1375-1381.
Haas, F., Gorb, S. and Wootton, R. J. (2000b). Elastic joints in dermapteran hind wings: materials and wing folding. *Arthropod Struct. Dev.* **29**, 137-146.
Heide, G. and Götz, K. G. (1996). Optomotor control of course and altitude in *Drosophila* is achieved by at least three pairs of flight steering muscles. *J. Exp. Biol.* **199**, 1711-1726.
Ho, S., Nassef, H., Pornsinsirirak, N., Tai, Y.-C. and Ho, C.-M. (2003). Unsteady aerodynamics and flow control for flapping wing flyers. *Prog. Aerospace Sci.* **39**, 635-681.
Jensen, M. and Weis-Fogh, T. (1962). Biology and physics of locust flight. V. Strength and elasticity of locust cuticle. *Philos. Trans. R. Soc. B Biol. Sci.* **245**, 137-169.
Lehmann, F.-O. and Götz, K. G. (1996). Activation phase ensures kinematic efficacy in flight-steering muscles of *Drosophila melanogaster*. *J. Comp. Physiol. A* **179**, 311-322.
Lehmann, F.-O., Gorb, S., Nasir, N. and Schützner, P. (2011). Elastic deformation and energy loss of flapping fly wings. *J. Exp. Biol.* **214**, 2949-2961.
Liu, W., Xiao, Q. and Cheng, F. (2013). A bio-inspired study on tidal energy extraction with flexible flapping wings. *Bioinspir. Biomim.* **8**, 036011.
Lv, S., Dudek, D. M., Cao, Y., Balamurali, M. M., Gosline, J. and Li, H. (2010). Designed biomaterials to mimic the mechanical properties of muscles. *Nature* **465**, 69-73.
Miyan, J. A. and Ewing, A. W. (1985). How Diptera move their wings: a re-examination of the wing base articulation and muscle systems concerned with flight. *Philos. Trans. R. Soc. B Biol. Sci.* **311**, 271-302.
Mountcastle, A. M. and Combes, S. A. (2013). Wing flexibility enhances load-lifting capacity in bumblebees. *Proc. R. Soc. B Biol. Sci.* **280**, 20130531.
Mountcastle, A. M. and Combes, S. A. (2014). Biomechanical strategies for mitigating collision damage in insect wings: structural design versus embedded elastic materials. *J. Exp. Biol.* **217**, 1108-1115.
Mountcastle, A. M. and Daniel, T. L. (2009). Aerodynamic and functional consequences of wing compliance. *Exp. Fluids* **46**, 873-882.
Newman, D. J. S. and Wootton, R. J. (1986). An approach to the mechanics of pleating in dragonfly wings. *J. Exp. Biol.* **125**, 361-372.
Senda, K., Obara, T., Kitamura, M., Yokoyama, N., Hirai, N. and Iima, M. (2012). Effects of structural flexibility of wings in flapping flight of butterfly. *Bioinspir. Biomim.* **7**, 025002.
Shyy, W., Lian, Y., Tang, J., Liu, H., Trizila, O., Stanford, B., Bernal, L., Cesnik, C., Friedmann, P. and Ifju, P. (2008). Computational aerodynamics of low Reynolds number plunging, pitching and flexible wings for MAV applications. *Acta Mech. Sinica* **24**, 351-373.
Tu, M. S. and Dickinson, M. H. (1996). The control of wing kinematics by two steering muscles of the blowfly (*Calliphora vicina*). *J. Comp. Physiol. A* **178**, 813-830.
Vanella, M., Fitzgerald, T., Preidikman, S., Balaras, E. and Balachandran, B. (2009). Influence of flexibility on the aerodynamic performance of a hovering wing. *J. Exp. Biol.* **212**, 95-105.
Vogel, S. (1967). Flight in *Drosophila* III. Aerodynamic characteristics of fly wings and wing models. *J. Exp. Biol.* **46**, 431-443.
Walker, S. M., Thomas, A. L. R. and Taylor, G. K. (2009). Deformable wing kinematics in the desert locust: how and why do camber, twist and topography vary through the stroke? J. *R. Soc. Interface* **6**, 735-747.
Weis-Fogh, T. (1960). A rubber-like protein in insect cuticle. *J. Exp. Biol.* **37**, 889-907.
Weis-Fogh, T. (1973). Quick estimates of flight fitness in hovering animals, including novel mechanisms for lift production. *J. Exp. Biol.* **59**, 169-230.
Wisser, A. and Nachtigall, W. (1984). Functional-morphological investigations on the flight muscles and their insertion points in the blowfly *Calliphora erythrocephala* (Insecta, Diptera). *Zoomorphology* **104**, 188-195.
Wootton, R. J. (1981). Support and deformability in insect wings. *J. Zool.* **193**, 447-468.
Wootton, R. J. (1992). Functional morphology of insect wings. *Annu. Rev. Entomol.* **37**, 113-140.
Wootton, R. J. (1995). Geometry and mechanics of insect hindwing fans: a modelling approach. *Proc. R. Soc. B Biol. Sci.* **262**, 181-187.
Wootton, R. J., Evans, K. E., Herbert, R. and Smith, C. W. (2000). The hind wing of a desert locust (*Schistocerca gregaria* Forskål). I. Functional morphology and mode of operation. *J. Exp. Biol.* **203**, 2945-2955.
Wootton, R. J., Herbert, R. C., Young, P. G. and Evans, K. E. (2003). Approaches to the structural modelling of insect wings. *Philos. Trans. R. Soc. B Biol. Sci.* **358**, 1577-1587.
Young, J., Walker, S. M., Bomphrey, R. J., Taylor, G. K. and Thomas, A. L. R. (2009). Details of insect wing design and deformation enhance aerodynamic function and flight efficiency. *Science* **325**, 1549-1552.
Zhao, L., Huang, Q., Deng, X. and Sane, P. S. (2010). Aerodynamic effects of flexibility in flapping wings. *J. R. Soc. Interface* **7**, 485-497.
Zhu, Q. (2007). Numerical simulation of a flapping foil with chordwise or spanwise flexibility. *AIAA J.* **45**, 2448-2457.

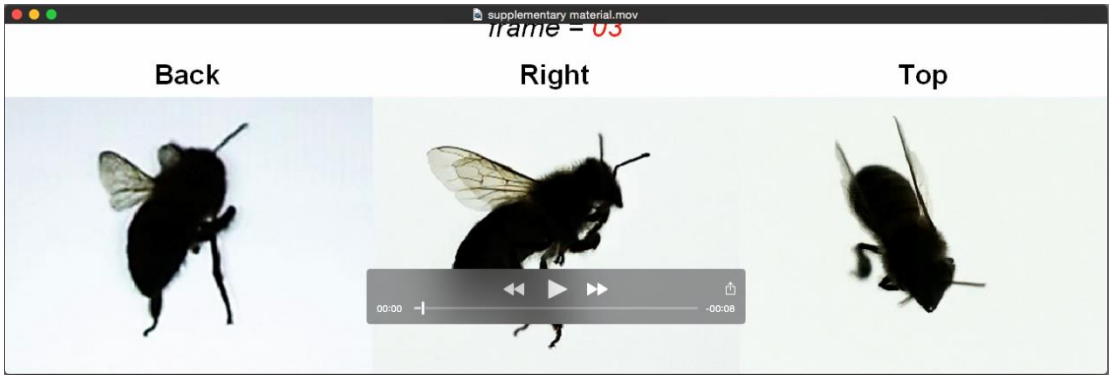

Movie 1. Synchronous wing deformation of three orthogonal views of the honeybee during free flapping flight, i.e. back view, right view and top view.